Appl Phys A (2008) 92: 773–776
DOI 10.1007/s00339-008-4572-5

Applied Physics A
Materials Science & Processing

Enhanced scattering efficiencies in spherical particles with weakly dissipating anisotropic materials

B.S. Luk'yanchuk · Cheng-Wei Qiu

Received: 12 October 2007 / Accepted: 4 March 2008 / Published online: 17 May 2008

Abstract This paper discusses light scattering by a small spherical particle with low dissipation rate and radial anisotropy in optical and magnetic properties, according to the extension of the Mie theory to the diffraction by an anisotropic sphere. It is shown that near plasmon (polariton) resonance frequencies anisotropy can lead to an additional increase in field enhancement.

PACS 42.25.Fx · 42.65.Es · 46.40.Ff · 78.67.Bf

1 Introduction

Ablation with nanoscale spatial resolution needs a special tool to localize spot size on the scale below 100 nm. A few methods were suggested for this purpose. The first method is related to light focusing with high numerical aperture lenses and the so-called subdiffractive optics, e.g. radially polarized light, Bessel-Gaussian beams, etc. [1–4]. The second method is to use field enhancement by a laser-illuminated tip (AFM tip, SEM tip, etc.), see e.g. [5–7]. The third method is related to application of the scanning near-field optical microscopy (SNOM) technique [8, 9]. Broad attention has also been given to optical resonances and near-field effects with transparent particles [10–12]. Last but not least, we should mention the method that uses field enhancement by plasmonic nanoparticles [13–16].

Although all these methods permit us to localize laser ablation on the scale below 100 nm, plasmonic particles are of special interest for many plasmonic nanodevices [17], biochemical applications [18], surface-enhanced Raman scattering [19], etc. The majority of experimental works and theoretical calculations were done with gold, silver and platinum nanoparticles which have sufficiently big dissipation near plasmon resonance frequencies. However, it is clear that higher field enhancement effects can be seen in materials with weak dissipation. This examination was done in [20–25] for isotropic materials. It was shown that materials with weak dissipation have a lot of peculiarities in light scattering. For example, Rayleigh scattering in these materials is replaced by anomalous light scattering with inverse hierarchy of optical resonances [22]; they demonstrated an extraordinary scattering effect [25] that is similar to quantum scattering by a potential with quasi-discrete levels and exhibits Fano resonances [26], etc. Similar effects can be seen during light scattering by nanowires [27] and, in principal, in any nanostructures with localized plasmons.

New effects may arise in anisotropic materials. Scattering of light by such anisotropic materials was previously analyzed in [28–32]. For this paper, we applied a modified Mie theory for theoretical investigation of light scattering near plasmon resonance frequencies.

2 Theoretical model

Following [32], we consider the material with radial anisotropies. In [32], the authors directly equated the radial components of electric and magnetic fields in the Maxwell equa-

B.S. Luk'yanchuk (✉)
Data Storage Institute, Agency for Science, Technology and Research, 117608 Singapore, Singapore
e-mail: Boris_L@dsi.a-star.edu.sg

C.-W. Qiu
Department of Electrical and Computer Engineering, National University of Singapore, Kent Ridge, 119260 Singapore, Singapore
e-mail: eleqc@nus.edu.sg

tions to obtain the anisotropic wave potentials. However, we prefer to start from rigorous Mie theory. We will discuss anisotropic spheres characterized by constitutive tensors of permittivity and permeability

$$\varepsilon = \begin{bmatrix} \varepsilon_r & 0 & 0 \\ 0 & \varepsilon_t & 0 \\ 0 & 0 & \varepsilon_t \end{bmatrix} \quad \text{and} \quad \mu = \begin{bmatrix} \mu_r & 0 & 0 \\ 0 & \mu_t & 0 \\ 0 & 0 & \mu_t \end{bmatrix}. \tag{1}$$

As usual, light scattering by a spherical particle can be expressed through Debye potentials (see, e.g. [33]). For the material with ε and μ given by (1), the electric ψ_{TM} and magnetic ψ_{TE} Debye potentials are presented by

$$\begin{aligned} &\frac{\varepsilon_r}{\varepsilon_t}\frac{\partial^2 \psi_{TM}}{\partial r^2} + \frac{1}{r^2 \sin\theta}\frac{\partial}{\partial\theta}\left(\sin\theta \frac{\partial \psi_{TM}}{\partial\theta}\right) \\ &\quad + \frac{1}{r^2\sin^2\theta}\frac{\partial^2\psi_{TM}}{\partial\varphi^2} + k_0^2\varepsilon_r\mu_t\psi_{TM} = 0, \\ &\frac{\mu_r}{\mu_t}\frac{\partial^2 \psi_{TE}}{\partial r^2} + \frac{1}{r^2 \sin\theta}\frac{\partial}{\partial\theta}\left(\sin\theta \frac{\partial \psi_{TE}}{\partial\theta}\right) \\ &\quad + \frac{1}{r^2\sin^2\theta}\frac{\partial^2\psi_{TE}}{\partial\varphi^2} + k_0^2\varepsilon_t\mu_r\psi_{TE} = 0. \end{aligned} \tag{2}$$

Here $k_0 = 2\pi/\lambda$ is the wave vector in vacuum. For isotropic materials, (2) converts into a usual wave equation. Solving these equations with corresponding boundary conditions one can find normalized scattering amplitudes a_ℓ (electric) and b_ℓ (magnetic):

$$a_\ell = \frac{n_t\psi'_\ell(q)\psi_{\nu_1}(n_t q) - \mu_t\psi_\ell(q)\psi'_{\nu_1}(n_t q)}{n_t\zeta'_\ell(q)\psi_{\nu_1}(n_t q) - \mu_t\zeta_\ell(q)\psi'_{\nu_1}(n_t q)}, \tag{3}$$

$$b_\ell = \frac{n_t\psi_\ell(q)\psi'_{\nu_2}(n_t q) - \mu_t\psi'_\ell(q)\psi_{\nu_2}(n_t q)}{n_t\zeta_\ell(q)\psi'_{\nu_2}(n_t q) - \mu_t\zeta'_\ell(q)\psi_{\nu_2}(n_t q)}, \tag{4}$$

where $n_t = \sqrt{\varepsilon_t\mu_t}$ is the complex refractive index and functions $\psi_\nu(x)$ and $\zeta_\ell(x)$ are given by

$$\psi_\nu(x) = \sqrt{\frac{\pi x}{2}} J_{\nu+\frac{1}{2}}(x), \qquad \zeta_\ell(x) = \sqrt{\frac{\pi x}{2}} H^{(1)}_{\ell+\frac{1}{2}}(x). \tag{5}$$

Functions $J_\ell(x)$ and $H^{(1)}_\ell(x)$ are usual Bessel and Hankel functions. The primes in (3)–(4) indicate differentiation with respect to the entire argument of the corresponding function, i.e. $\psi'_\ell(x) = \frac{d\psi_\ell(x)}{dx}$, etc. The value $q = k_0 a$ presents the so-called Mie size parameter, and a is the particle radius. Formulas (3)–(4) look quite similar to the usual ones of the Mie theory [33]. One can see from these formulas that all the information about particle anisotropy is presented by the order of spherical Bessel functions [28, 32]:

$$\nu_1 = \nu_1(\ell) = \left[\ell(\ell+1)A_e + \frac{1}{4}\right]^{1/2} - \frac{1}{2}, \quad A_e = \frac{\varepsilon_t}{\varepsilon_r}, \tag{6}$$

and

$$\nu_2 = \nu_2(\ell) = \left[\ell(\ell+1)A_m + \frac{1}{4}\right]^{1/2} - \frac{1}{2}, \quad A_m = \frac{\mu_t}{\mu_r}. \tag{7}$$

With $A_e = A_m = 1$, we have $\nu_1 = \nu_2 = \ell$ which returns to standard formulas of the Mie theory. Extinction, scattering, and absorption efficiencies are expressed through scattering amplitudes in the usual way [33]:

$$\begin{aligned} Q_{ext} &= \frac{2}{q^2}\sum_{\ell=1}^{\infty}(2\ell+1)\,\mathrm{Re}(a_\ell + b_\ell), \\ Q_{sca} &= \frac{2}{q^2}\sum_{\ell=1}^{\infty}(2\ell+1)\{|a_\ell|^2 + |b_\ell|^2\}, \\ Q_{abs} &= Q_{ext} - Q_{sca}. \end{aligned} \tag{8}$$

In practical detection problems, the so-called radar backscattering cross-section (RBS) is of great interest. This cross-section is presented by

$$Q_{RBS} = \frac{1}{q^2}\left|\sum_{\ell=1}^{\infty}(2\ell+1)(-1)^\ell(a_\ell - b_\ell)\right|^2. \tag{9}$$

Thus, we investigate peculiarities of light scattering by a small anisotropic particle near plasmon resonance frequencies. First, we want to present coefficients in (3)–(4) in a more convenient form

$$a_\ell = \frac{\Re^{(a)}_\ell}{\Re^{(a)}_\ell + i\Im^{(a)}_\ell}, \qquad b_\ell = \frac{\Re^{(b)}_\ell}{\Re^{(b)}_\ell + i\Im^{(b)}_\ell}, \tag{10}$$

where $\Re_\ell$ and $\Im_\ell$ functions are given by

$$\begin{aligned} \Re^{(a)}_\ell &= n_t\psi'_\ell(q)\psi_{\nu_1}(n_t q) - \mu_t\psi_\ell(q)\psi'_{\nu_1}(n_t q), \\ \Im^{(a)}_\ell &= n_t\chi'_\ell(q)\psi_{\nu_1}(n_t q) - \mu_t\psi'_{\nu_1}(n_t q)\chi_\ell(q), \\ \Re^{(b)}_\ell &= n_t\psi_\ell(q)\psi'_{\nu_2}(n_t q) - \mu_t\psi'_\ell(q)\psi_{\nu_2}(n_t q), \\ \Im^{(b)}_\ell &= n_t\chi_\ell(q)\psi'_{\nu_2}(n_t q) - \psi_{\nu_2}(n_t q)\chi'_\ell(q). \end{aligned} \tag{11}$$

Here $\chi_\ell(x) = \sqrt{\frac{\pi x}{2}} N_{\ell+\frac{1}{2}}(x)$, where $N_\ell(x)$ is the Neumann function. The scattering amplitudes a_ℓ and b_ℓ depend on parameter q and the real and imaginary parts of the dielectric permittivities $\varepsilon_r, \varepsilon_t$ and permeabilities μ_r and μ_t. To simplify further consideration we'll discuss the nonmagnetic media with $\mu_r = \mu_t = 1$ and, additionally, consider the limiting case of nondissipative media, where $\mathrm{Im}\,\varepsilon_r = \mathrm{Im}\,\varepsilon_t = 0$. For this case the scattering amplitudes depend on three parameters: $\mathrm{Re}\,\varepsilon_r$, $\mathrm{Re}\,\varepsilon_t$ and q. For fixed ε_r and ε_t amplitudes a_ℓ and b_ℓ oscillate versus size parameter q. They reach maximal values at some points (the so-called optical resonances [33]). One can see immediately from (10)–(11)

that, for nondissipative media, maximal values of amplitudes are $a_\ell = 1$ and $b_\ell = 1$. They are reached at the points where $\Im_\ell^{(a)}(q, \varepsilon) = 0$ and $\Im_\ell^{(b)}(q, \varepsilon) = 0$, respectively. These equations present the trajectories of optical resonances on $\{q, \varepsilon\}$ plane. There are two different branches of optical resonances. The first one is related to usual Mie resonances which are associated with excitation of volume waves in the spherical cavity [33]. These resonances typically arise at rather large values of the size parameter $q > 1$ and for this case resonances of electric and magnetic amplitudes are overlapped. Another branch is associated with excitation of surface electromagnetic waves (plasmons). For isotropic case these resonances at the limit of small particle $q \to 0$ occur in electrical amplitudes a_ℓ at $\varepsilon = \varepsilon_\ell = -(\ell + 1)/\ell$. One can see in Fig. 1, that the anisotropy influenced the positions of surface optical resonances while positions of volume resonances remain practically unchanged.

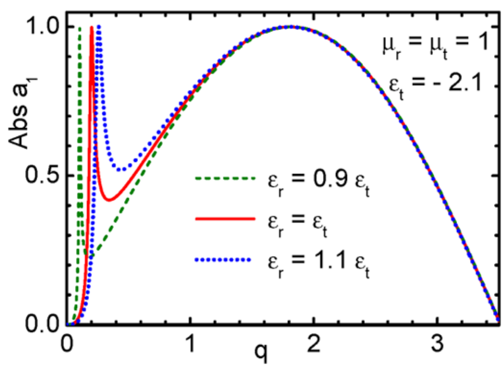

Fig. 1 Variation of surface plasmon resonance (for dipole mode $\ell = 1$) versus the particle size at different anisotropies

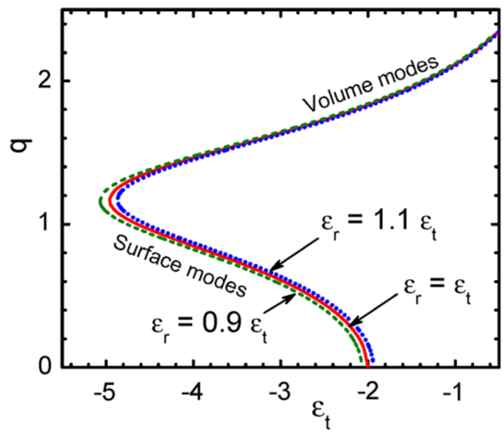

Fig. 2 Variation of the dipole resonance trajectory for different anisotropies. We consider the same values of ε and μ as in Fig. 1

In Fig. 2 we show the variation of the dipole electric resonance $a_1(\varepsilon_r, \varepsilon_t, q) = 1$ trajectory for different anisotropies. As we mentioned, the anisotropy mainly influenced positions of the surface modes. Both values of ε_r and ε_t in Fig. 2 are negative. One can see that for fixed ε_t value surface plasmon resonance moves into the smaller q values with $\varepsilon_r/\varepsilon_t < 1$ and into the larger q values in the opposite situation with $\varepsilon_r/\varepsilon_t > 1$.

As one can see in (8)–(9), the scattering efficiencies are inversely proportional to q^2, thus, a shift in the resonance positions strongly influences the scattering efficiencies, as shown in Fig. 3. With a 10% variation of anisotropy parameter we have a variation of the resonant value of q about two to three times which, in turn, leads to a variation of the scattering efficiencies by an order of magnitude.

Thus, we can see that even a small variation in the anisotropy plays an important role in enhancing or prohibiting scattering efficiencies. It can be shown that similar variations arise in the field enhancement also. However, it is necessary to emphasize that such a big impact due to radial anisotropy can *only* be seen in nondissipating materials. With dissipation (both in ε_t or in ε_r), this enhancement becomes less pronounced. Anisotropy may lead to some unusual effects, e.g. nonzero absorption $Q_{abs} \neq 0$ within

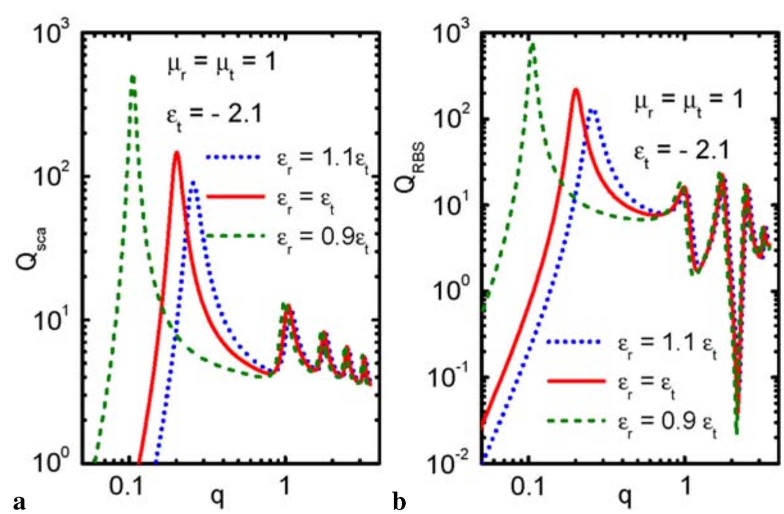

Fig. 3 Scattering efficiencies associated with surface plasmon resonances

nondissipative $\mathrm{Im}\,\varepsilon_{r,t} = 0$ and nonmagnetic $\mu_{r,t} = 1$ materials with opposite signs of dielectric permittivities $\varepsilon_r > 0$ and $\varepsilon_t < 0$.

Having in mind the practical realization of the anisotropy effect we should mention the graphitic multishell structures [34], spherically stratified medium [35], and indeed the cell membranes containing mobile charges [36].

3 Conclusion

We demonstrated theoretically that the anisotropy can additionally enhance the surface plasmon resonance effect, when both ε_r and ε_t are negative and $|\varepsilon_r| < |\varepsilon_t|$. A corresponding field enhancement in weakly dissipating materials can reach about the order of magnitude for small particles.

References

1. R. Dorn, S. Quabis, G. Leuchs, Phys. Rev. Lett. **91**, 233901 (2003)
2. Y. Kozawa, S. Sato, Opt. Lett. **30**, 3063 (2005)
3. Y. Kozawa, S. Sato, Opt. Lett. **31**, 820 (2006)
4. H.F. Wang, L.P. Shi, B.S. Luk'yanchuk, C.J.R. Sheppard, T.C. Chong, G. Yuan, arXiv:0709.2748v1 [physics.pop-ph] (18 September 2007)
5. S.M. Huang, M.H. Hong, Y.F. Lu, B.S. Luk'yanchuk, W.D. Song, T.C. Chong, J. Appl. Phys. **91**, 3268 (2002)
6. R.M. Roth, N.C. Panoiu, M.M. Adams, R.M. Osgood Jr., C.C. Neacsu, M.B. Raschke, Opt. Express **14**, 2921 (2006)
7. Z.B. Wang, B.S. Luk'yanchuk, L. Li, P.L. Crouse, Z. Liu, G. Dearden, K.G. Watkins, Appl. Phys. A **89**, 363 (2007)
8. L. Vaccaro, L. Aeschimann, U. Staufer, H.P. Herzig, R. Dändliker, Appl. Phys. Lett. **83**, 584 (2003)
9. M.H. Hong, Y. Lin, G.X. Chen, L.S. Tan, Q. Xie, B. Luk'yanchuk, L.P. Shi, T.C. Chong, J. Phys.: Conf. Ser. **59**, 64 (2007)
10. H.-J. Münzer, M. Mosbacher, M. Bertsch, O. Dubbers, F. Burnmeister, A. Park, R. Wannemather, B.-U. Runge, D. Bäuerle, J. Boneberg, P. Leiderer, Proc. SPIE **4426**, 180 (2002)
11. B.S. Luk'yanchuk, Z.B. Wang, W.D. Song, M.H. Hong, Appl. Phys. A **79**, 747 (2004)
12. N. Arnold, G. Schrems, D. Bäuerle, Appl. Phys. A **79**, 729 (2004)
13. A. Plech, V. Kotaidis, M. Lorenc, J. Boneberg, Nat. Phys. **2**, 44 (2006)
14. N. Nedyalkov, T. Sakai, T. Miyanishi, M. Obara, J. Phys. D: Appl. Phys. **39**, 5037 (2006)
15. N. Nedyalkov, T. Sakai, T. Miyanishi, M. Obara, Appl. Phys. Lett. **90**, 123106 (2007)
16. D. Eversole, B. Luk'yanchuk, A. Ben-Yakar, Appl. Phys. A **89**, 283 (2007)
17. W.L. Barnes, A. Dereux, T.W. Ebbesen, Nature **424**, 824 (2003)
18. E.M. Goldys, A. Barnett, F. Xie, K. Drozdowicz-Tomsia, I. Gryczynski, E.G. Matveeva, Z. Gryczynski, T. Shtoyko, Appl. Phys. A **89**, 265 (2007)
19. Z.B. Wang, B. Luk'yanchuk, W. Guo, S. Edwardson, D.J. Whitehead, L. Li, Z. Liu, K.G. Watkins, J. Chem. Phys. **128**, 094705 (2008)
20. Z.B. Wang, B.S. Luk'yanchuk, M.H. Hong, Y. Lin, T.C. Chong, Phys. Rev. B **70**, 032427 (2004)
21. B.S. Luk'yanchuk, M.I. Tribelsky, V. Ternovsky, J. Opt. Technol. **73**, 371 (2006)
22. M.I. Tribelsky, B.S. Luk'yanchuk, Phys. Rev. Lett. **97**, 263902 (2006)
23. B.S. Luk'yanchuk, Z.B. Wang, M. Tribelsky, V. Ternovsky, M.H. Hong, T.C. Chong, J. Phys.: Conf. Ser. **59**, 234 (2007)
24. B.S. Luk'yanchuk, M.I. Tribelsky, V. Ternovsky, Z.B. Wang, M.H. Hong, L.P. Shi, T.C. Chong, J. Opt. A: Pure Appl. Opt. **9**, S294 (2007)
25. B.S. Luk'yanchuk, M.I. Tribelsky, Z.B. Wang, Y. Zhou, M.H. Hong, L.P. Shi, T.C. Chong, Appl. Phys. A **89**, 259 (2007)
26. M.I. Tribelsky, S. Flach, A.E. Miroshnichenko, A. Gorbach, Yu.S. Kivshar, Phys. Rev. Lett. **100**, 043903 (2008)
27. B.S. Luk'yanchuk, V. Ternovsky, Phys. Rev. B **73**, 235432 (2006)
28. K.-L. Wong, H.-T. Chen, IEE Proc. H Microw. Antennas Propag. **139**, 314 (1992)
29. B. Stout, M. Nevière, E. Popov, J. Opt. Soc. Am. A **23**, 1111 (2006)
30. B. Stout, M. Nevière, E. Popov, J. Opt. Soc. Am. A **23**, 1124 (2006)
31. B. Stout, M. Nevière, E. Popov, J. Opt. Soc. Am. A **24**, 1120 (2007)
32. C.-W. Qiu, L.-W. Li, T.-S. Yeo, S. Zouhdi, Phys. Rev. E **75**, 026609 (2007)
33. M. Born, E. Wolf, *Principles of Optics*, 7th edn. (University Press, Cambridge, 1999)
34. A.A. Lucas, L. Henrard, Ph. Lambin, Phys. Rev. B **49**, 2888 (1994)
35. J.C.E. Sten, IEEE Trans. Dielectr. Electr. Insul. **2**, 360 (1995)
36. V.L. Sukhorukov, G. Meedt, M. Kurschner, U. Zimmermann, J. Electrost. **50**, 191 (2001)